



National Environmental Science Programme

# Coastal change detection tools utilising 28 years of Earth Observation data in the Australian Geoscience Data Cube (AGDC)

Stephen Sagar<sup>1</sup>, Peter Tan<sup>1</sup>, Leo Lymburner<sup>1</sup> & Dale Roberts<sup>1,2</sup>

<sup>1</sup>Geoscience Australia, <sup>2</sup>Australian National University

Understanding pressures on the marine environment

March 2016





Enquiries should be addressed to:  
Dr Stephen Sagar  
stephen.sagar@ga.gov.au

## Copyright

This report is licensed by the University of Tasmania for use under a Creative Commons Attribution 4.0 Australia Licence. For licence conditions, see <https://creativecommons.org/licenses/by/4.0/>

## Acknowledgement

This work was undertaken for the Marine Biodiversity Hub, a collaborative partnership supported through funding from the Australian Government's National Environmental Science Programme (NESP). NESP Marine Biodiversity Hub partners include the University of Tasmania; CSIRO, Geoscience Australia, Australian Institute of Marine Science, Museum Victoria, Charles Darwin University, the University of Western Australia, Integrated Marine Observing System, NSW Office of Environment and Heritage, NSW Department of Primary Industries.

## Important Disclaimer

The NESP Marine Biodiversity Hub advises that the information contained in this publication comprises general statements based on scientific research. The reader is advised and needs to be aware that such information may be incomplete or unable to be used in any specific situation. No reliance or actions must therefore be made on that information without seeking prior expert professional, scientific and technical advice. To the extent permitted by law, the NESP Marine Biodiversity Hub (including its host organisation, employees, partners and consultants) excludes all liability to any person for any consequences, including but not limited to all losses, damages, costs, expenses and any other compensation, arising directly or indirectly from using this publication (in part or in whole) and any information or material contained in it.

# Contents

<b>Executive Summary .....</b>	<b>3</b>
<b>1. Introduction .....</b>	<b>3</b>
1.1 The Australian Geoscience Data Cube (AGDC).....	4
1.2 Aims and Scope of this Report .....	5
<b>2. Water detection from time series data .....</b>	<b>5</b>
2.1 Water Observations from Space (WOfS).....	5
2.2 Water Detection in the Intertidal & Coastal Zone.....	6
2.3 The Random Forest time-series approach .....	6
<b>3. Time-series Change Detection .....</b>	<b>7</b>
3.1 Example of Output – Brisbane Port, Moreton Bay QLD .....	8
3.2 Visualising identified areas of change .....	9
3.2.1 Moreton Bay, QLD .....	10
3.2.2 Murray Mouth & Lower Lakes, SA.....	16
<b>4. Future Work &amp; Linkages .....</b>	<b>20</b>
4.1 Extension to other Variables .....	20
4.2 Developing Data Sets to support Coastal Applications .....	22
<b>5. Conclusions.....</b>	<b>23</b>
<b>REFERENCES.....</b>	<b>24</b>
<b>Appendix A .....</b>	<b>26</b>

## List of Figures

Figure 1 – The 1° by 1° cells in the current version of the Australian Geoscience Data Cube (AGDC)	4
Figure 2 – Example of a Probabilistic Water Classification Output for one pixel through the time series, showing the widely varying random forest probability of water classification at each time epoch, characteristic of an intertidal area.	7
Figure 3 – Conceptual Diagram of the Sliding Window Change Detection Approach	8
Figure 4 – Brisbane Port - 95% Probability of change from Water to Dry including the estimated date of change	9
Figure 5 – Moreton Bay, QLD – Study Sites for Change Detection	10
Figure 6 – Southern Moreton Island - 95% Probability of Change areas for Water to Dry, Dry to Water and Multiple Changes. Sample Point locations for multiple (A) and intertidal (B) change analysis.	11
Figure 7 – Pixel Drill at Sample Point A showing Probability of Water detection through the time-series.	12
Figure 8 - Pixel Drill at Sample Point B showing Probability of Water detection through the time-series	12
Figure 9 – Southern Stradbroke Island – 95% Probability of Change from Water to Dry and estimated change dates.	13
Figure 10 - Pixel Drill at Sample Point C showing Probability of Water detection through the time-series	14
Figure 11 - Southern Stradbroke Island – 95% Probability of Change from Dry to Water and estimated change dates.	15
Figure 12 - Pixel Drill at Sample Point D showing Probability of Water detection through the time-series	15
Figure 13 – The Murray Mouth and Lower Lakes Region – 95% Probability of Change regions shown along with the estimated time of change. Transects for further analysis shown over the Murray Mouth and Ewe Island Barrage at Lake Alexandrina	16
Figure 14 – Hovmöller Diagram of the Ewe Island Barrage Transect. Low NDWI values (red) indicate Land, through to high values (blue) indicating water.	18
Figure 15 – River Flow Data at River Murray Lock One Downstream – Megalitres per Day.	18
Figure 16 - Hovmöller Diagram of the Murray Mouth Transect. Low NDWI values (red) indicate Land, through to high values (blue) indicating water	19
Figure 17 – Junction Bay mangrove community stripped and flattened, post TC Monica– Photo Credit: Garry Cook, CSIRO Sustainable Ecosystems	20
Figure 18 - Hovmöller Diagram of the Junction Bay Mangrove Community, NT. High NDVI values (green) indicate healthy vegetation, through to yellow which is indicative of soil or damaged vegetation, through to blue indicating water.	21
Figure 19 – Low (left) and High (right) tide composite reflectance images derived from modelled tides across 20 years of Landsat data in the Kimberley Region, WA.	22



---

## EXECUTIVE SUMMARY

The ability to detect, measure and monitor change in coastal and marine environments can assist in both informing management decision processes and evaluating the results of management interventions. Change detection utilising satellite data requires robust time-series data at temporal and spatial scales that can provide context for meaningful interpretations of coastal and marine ecosystem processes. Previously, this analysis has employed time consuming methods that hampered the efficient extraction of key information on environmental change and trends.

The recently developed Australian Geoscience Data Cube (AGDC) provides a quantum step forward in our ability to utilise satellite data for environmental monitoring. The AGDC provides a platform for efficient processing and analysis of these data, enabling quantitative information to be extracted from the full 28-year time series of the Landsat data archive. Also, this approach can be applied to a wide range of current and future satellite data streams (e.g. Sentinel series of satellites) to provide rapid, robust environmental monitoring.

We have developed a flexible diagnostic change detection tool, able to extract change events from classified variables derived from 28 years of Landsat data in the AGDC. In this report we describe how we apply the algorithm to a water detection problem, and show the broadscale application using examples of coastal change and estuarine drying events in Moreton Bay and the Murray Mouth and Lower Lakes. We also introduce tools which can then be used for further analysis of the detected change events.

The algorithm is flexible enough to be applied to a range of variables in the coastal zone, and we discuss further applications and potential future linkages to extend this work for the examination of important ecological communities.

## 1. INTRODUCTION

The ability to monitor and detect change in the coastal zone is valuable across a wide range of application areas including environmental monitoring, coastline change assessment, habitat mapping and scientific information to inform planning and policy.

Over the last three decades, remote sensing has been increasingly recognised as a fundamental and cost effective tool for tackling the broad spatial and temporal scales required for baseline monitoring and environmental change detection. Traditionally, this has meant analysis of an individual scene of a study area, or multiple scenes at a few specified time series epochs. Applications where this kind of approach has been used in the coastal zone are wide and varied, and include seagrass monitoring (Lyons et al., 2012), examining the extent change of intertidal flats (Murray et al., 2014), detecting coral bleaching events (Yamano and Tamura, 2004) and shoreline change analysis (Chen and Rau, 1998; White and El Asmar, 1999; Shetty et al., 2015).

In this report we examine a different kind of approach to change detection, utilising the full 28 year archive of Landsat imagery managed in the Australian Geoscience Data Cube (AGDC). Fundamentally, we are looking to explore the ability of the AGDC data to act as a diagnostic tool for detecting change.

In many change detection applications, often some knowledge of the expected timing and spatial locations of a change event is required to enable appropriate Earth Observation (EO) data to be selected for analysis. By utilising the AGDC, we look to move past this requirement, using the full 28 years of data to identify the regions and timing of potential changes, and allowing us to employ new tools to investigate these changes further.

## 1.1 The Australian Geoscience Data Cube (AGDC)

The Australian Geoscience Data Cube (AGDC) is a collaborative project between Geoscience Australia, CSIRO and the National Computational Infrastructure (NCI) established in 2014, resulting from the Australian Space Research Program funded 'Unlocking the Landsat Archive' initiative.

The AGDC provides an integrated gridded data analysis environment for decades of analysis-ready earth observation (EO) satellite data (<http://www.datacube.org.au/>). The 28 year archive of Landsat data over the Australian continent is processed to a standardised surface reflectance, accounting for atmospheric correction and terrain and viewing/illumination effects (Li et al., 2012), including pixel quality indicators to identify anomalies such as cloud or band saturation (Sixsmith et al., 2013).

The satellite image data is then spatially segmented into 1° by 1° cells to form a regular grid of temporal epoch tiles that covers Australia at a 25m pixel spatial resolution (Figure 1). The temporal frequency of the data acquisitions varies both spatially, and over the 28 year time period. Crucially, having tiles with a fixed and consistent footprint in a linked relational database provides a highly efficient structure for EO data analysis in a high performance computing environment such as the NCI (Lewis et al., 2015).

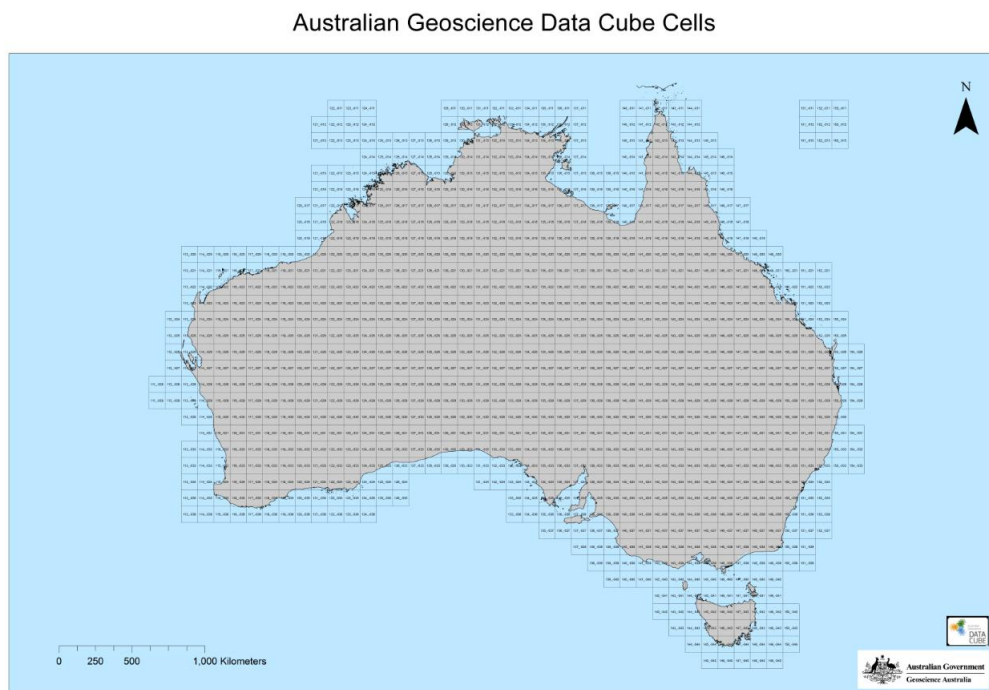


Figure 1 – The 1° by 1° cells in the current version of the Australian Geoscience Data Cube (AGDC)

## 1.2 Aims and Scope of this Report

The aim of this report is to investigate and illustrate some of the tools and methods for change detection that can be used when analysing the time series of EO data in the AGDC. This work extends classification work completed on a national scale to detect water in the coastal and inter-tidal zone.

We aim to demonstrate some of the broad-scale diagnostic tools that can be applied to the time-series classification to detect when change has occurred, and highlight the issues that must be dealt with in a dynamic region such as the coastal zone. This leads to the application of targeted tools, to examine in more detail the detected change events throughout the 28 year time period being analysed.

By applying these techniques to coastal/estuarine regions with a known change event, we highlight the potential of time-series analysis to semi-automatically extract spatial extents of change and to analyse the complex nature of the changes over time.

Focusing the scope of this study on a simple water/non-water classification allows us to illustrate the potential of these techniques for coastal change analysis, with the possibility of extending them in the future to other ecological variables that may be classified in the coastal zone (salt-marshes, mangroves, seagrass etc).

## 2. WATER DETECTION FROM TIME SERIES DATA

To demonstrate our approach to change detection, we focus on the well-studied remote sensing problem of the pixel-by-pixel detection of water (McFeeters, 1996; Xu, 2006; Fisher and Danaher, 2013; Fisher et al., 2016; Mueller et al., 2016; Tulbure et al., 2016). By doing so we are achieving two objectives. One, we are extending work already completed at Geoscience Australia in the Water Observations from Space (WOfS) project, and two, as essentially a classification problem, we are providing a framework for investigating change of other important environmental variables.

### 2.1 Water Observations from Space (WOfS)

The WOfS project has in many ways been the initial flagship application derived from the Landsat archive and the AGDC. WOfS is a continental scale pixel-based assessment of the presence and frequency of water across the full 28 year time series of the AGDC Landsat archive (Mueller et al., 2016).

The WOfS output product provides the number of times water has been observed at each pixel over the last 28 years, and provides a comprehensive snapshot of the continent, identifying the spatial extents of flooding events, seasonal inundation patterns and drought affected water storage extents ([http://eos-test.ga.gov.au/geoserver/www/remote\\_scripts/WOfS\\_v1.5.htm](http://eos-test.ga.gov.au/geoserver/www/remote_scripts/WOfS_v1.5.htm))

## 2.2 Water Detection in the Intertidal & Coastal Zone

Detecting water in the intertidal and coastal zone requires us to extend and vary the WOfS approach to deal with the specific nature of the environment. Essentially, the intertidal zone can be considered a short frequency periodic inundation event, in contrast to more episodic events dealt with in the terrestrial WOfS product, such as floods. This has implications for the composition and spectral reflectance of the 'land' surfaces exposed at a low tide epoch.

Many tidal flats at low tide still consist of shallow layers or a thin film of water, which can strongly effect the absorption of the Near Infra-Red (NIR) and Short Wave Infra-Red (SWIR) portions of the remote sensing reflectance signal (Brockmann and Stelzer, 2008). The sample set used in WOfS does not consist of these types of 'dry' samples, and applied to the intertidal zone will often classify them as water.

Additionally, as an application aimed at terrestrial water, the WOfS sample set does not contain many of the water types encountered in the aquatic zone. These can range from highly turbid sediment outflow waters to clear coral-reef waters with optical depth visibility up to 30m. Hence, the first step in moving the water classification algorithm to the approach detailed in section 2.3 was the manual acquisition of many thousands of representative spectral coastal and intertidal samples, from a variety of sites and Landsat images.

Many classification algorithms dealing with the water/non-water problem in the intertidal and coastal zone rely on a degree of manual interpretation or classification thresholding (Ryu et al., 2002; Murray et al., 2012), often to deal with the degree of uncertainty caused by different water types and remnant water on the tidal flats. To deal with this aspect of uncertainty, for which the decision tree approach in WOfS is ill-suited, we propose the use of a random forest classification approach.

## 2.3 The Random Forest time-series approach

The random forest (RF) classification approach (Ho, 1995; Breiman, 2001) is gaining in popularity, due to its robustness in dealing with noise and range of sample data, and its ability to represent classifications in a probabilistic framework. The RF approach constructs a number of decision trees based on the supplied sample data. Each of these trees only uses a subset of the sample data and of the sample decision variables in its construction.

In our remote sensing water problem, the decision variables may consist of the band values of the data, plus some other indices relevant to the problem such as the Normalised Difference Water Index (NDWI) (McFeeters, 1996) or Modified Difference Water Index (MDWI) (Xu, 2006). In our version of the random forest, each tree then votes with a probability of a pixel being water or not water, based on the subset of data and variables it has used. These votes are then combined to form a probability of water being present in the pixel.

As we step through the time series at each pixel, the RF model is applied, and we are able to generate a probabilistic assessment of the presence of water at each time epoch (Figure 2), rather than the binary water/not-water approach of the WOfS implementation.

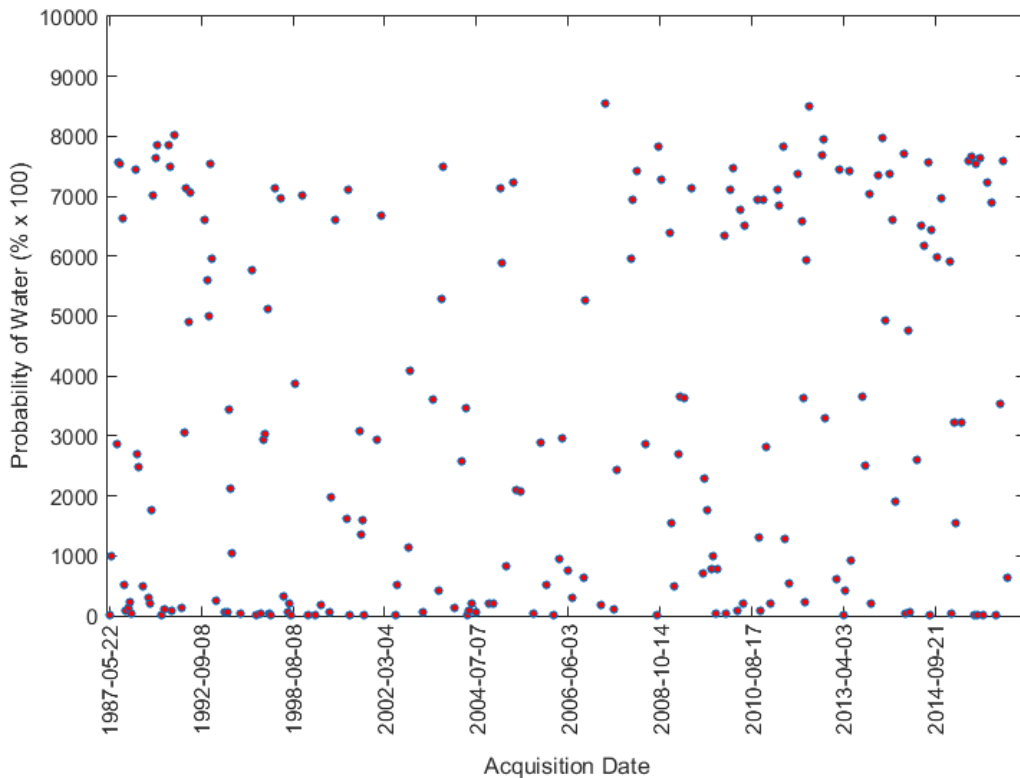


Figure 2 – Example of a Probabilistic Water Classification Output for one pixel through the time series, showing the widely varying random forest probability of water classification at each time epoch, characteristic of an intertidal area.

### 3. TIME-SERIES CHANGE DETECTION

In time series analysis, change detection is aimed at identifying times when the probability distribution of the time series changes. In remote sensing applications, one approach is to apply harmonic analysis models on a time series of spectral or a derivation of spectral values to detect phenological changes. BFAST (Verbesselt et al., 2010) is one example of such an approach.

Harmonic analysis models work well on remote sensing time series which show strong seasonal patterns. However, such a method is not good at detecting environmental change events which do not follow seasonal patterns, such as floods, bush fires, afforestation/deforestation, or in our case, coastal change.

In this report, we adopt another approach, which does not attempt to find the change point using spectral time series data directly. Instead, spectral data are feed into the random forest classification model to assign them a probabilistic water/non-water classification. As such, the time series of spectral data are converted to time series of probability based surface object classes.

The developed change detection algorithm then models the time series of objects or a set of coefficients derived from the time series (Tan et al., 2011). First, we define a function  $f(x, t, w)$  on a sliding window of the time series, where  $x$  is the time series data,  $t$  is the time value,  $w$  is the width of the window (Figure 3)

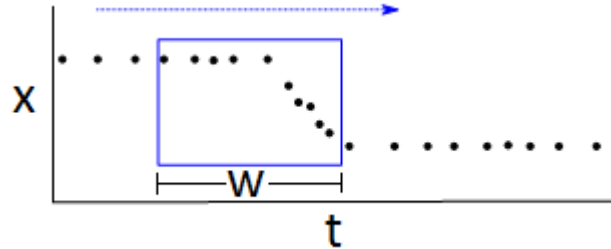


Figure 3 – Conceptual Diagram of the Sliding Window Change Detection Approach

Note  $f(x, t, w) \in (a, b)$  as  $f_{(a,b)}$ , then the posterior probability of a change event occurring is given by  $P(C|f_{(a,b)}) = \frac{P(f_{(a,b)}|C)P(C)}{P(f_{(a,b)})}$ . The prior probability of change is a constant of  $f_{(a,b)}$ , while  $P(f_{(a,b)}|C)$  can be estimated by a set of training samples provided to the RF algorithm construction, and  $P(f_{(a,b)}) = \frac{\sum_a^b I(f)}{\sum_{-\infty}^{+\infty} I(f)}$ .

In this project,  $f(x, t, w)$  is defined as  $\frac{W_l}{N_l+W_l} - \frac{W_r}{N_r+W_r}$ , where  $W_l$  and  $N_l$  is the number of water observations and non-water observation in the first half of the window respectively, while  $W_r$  and  $N_r$  is the number of water observations and non-water observation in the second half of the window respectively. As such,  $f(x) \in [-1,1]$ , with  $f(x) = 1$  corresponding to maximum probability of changing from wet to dry,  $f(x) = -1$  corresponding to maximum probability of changing from dry to wet and  $f(x) = 0$  corresponding to the minimum probability of any changes.

### 3.1 Example of Output – Brisbane Port, Moreton Bay QLD

To illustrate the concepts described in the algorithm, it is helpful to select a region with a known and distinct pattern of change. In terms of the detection of water, one of the easiest targets is an area where there has been the construction of man-made features such as wharves, jetties or land-reclamation for development. The example shown in Figure 4 has been chosen to show the ability of the algorithm to detect the step-wise construction of Brisbane Port in Moreton Bay, QLD (Figure 5, site A).

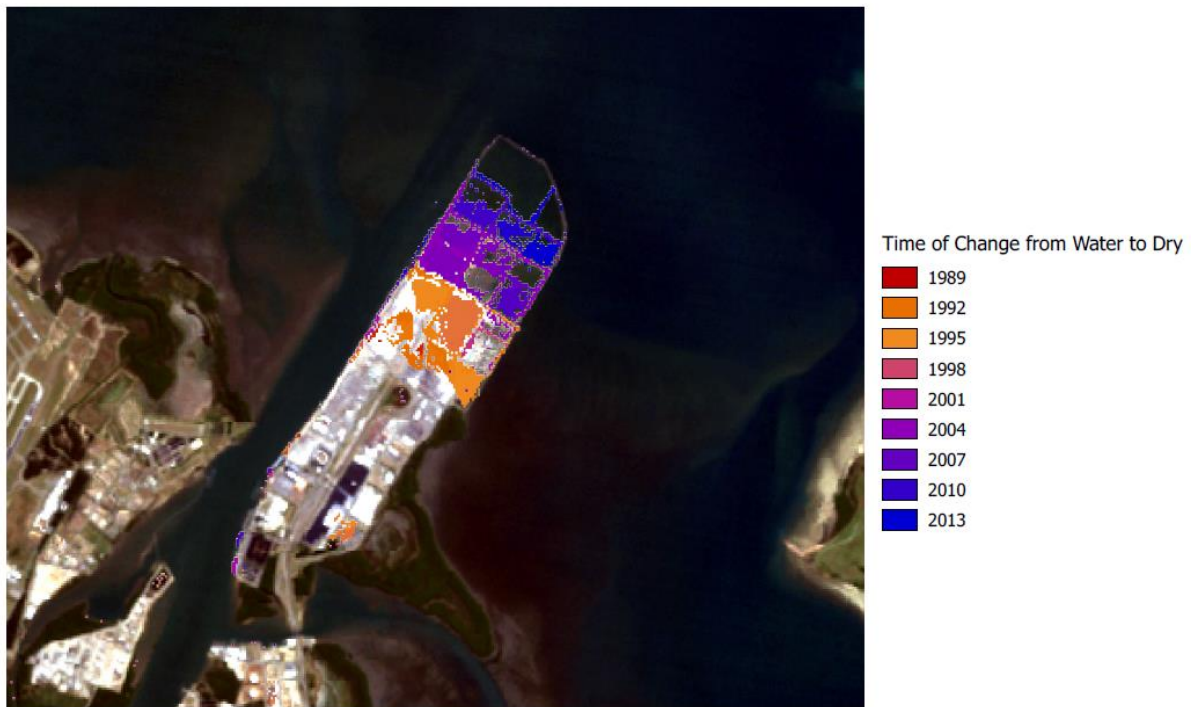


Figure 4 – Brisbane Port - 95% Probability of change from Water to Dry including the estimated date of change

In this test of the algorithm we have used a sliding time window length of 4 years ( $w=4$ ), meaning that we are detecting change that is persistent over that time period. By selecting the pixels in the output that have a probability of change of over 95%, we can determine the regions where we are quite sure we have observed change, in this case from wet to dry.

The algorithm then returns for each pixel the time value ( $t$ ) when the maximum probability of change was detected, allowing us to produce the extent and timing map shown in Figure 4. Here we can clearly see construction of the port infrastructure detected from the early 1990's through to more recent additions from 2010-13. Whilst this a simple example to illustrate the functionality of the algorithm, in the next section we show examples looking for more dynamic natural environmental change, and how other tools can then be employed to help understand the change we detect.

### 3.2 Visualising identified areas of change

In this section we examine the outputs of the change detection algorithm for two study area locations, Moreton Bay, QLD and the Murray Mouth and Lower Lakes Region, SA. These locations have been selected as they exhibit a number of distinct types of coastal and/or estuarine change, to which we can apply different types of interpretive tools to further analyse the outputs of the change detection algorithm.

### 3.2.1 Moreton Bay, QLD

Moreton Bay (Figure 5) is mostly enclosed by large sand islands, and consists of a diverse community of mangroves, mudflats, seagrass beds and hard and soft corals (Lyons et al., 2012). To examine coastal change, we have selected two sites, entrances to the bay at the southern tips of Moreton Island (Site B) and Stradbroke Island (Site C). At these sites we would expect to see a dynamic coastal environment of sand erosion and deposition over time that can test the detection capabilities of the algorithm.

One of the first challenges in working in a more dynamic coastal or tidal environment is being able to characterise the types of changes we detect, and isolate the more persistent episodic change events from the periodic change occurring in the inter-tidal zone. In a dynamic environment however, a single location may change many times over the time-series period. Shown in Figure 6, we use the detection of both types of change event, water-dry and dry-water, to show how we can distinguish between a single and multiple change events at study site B.

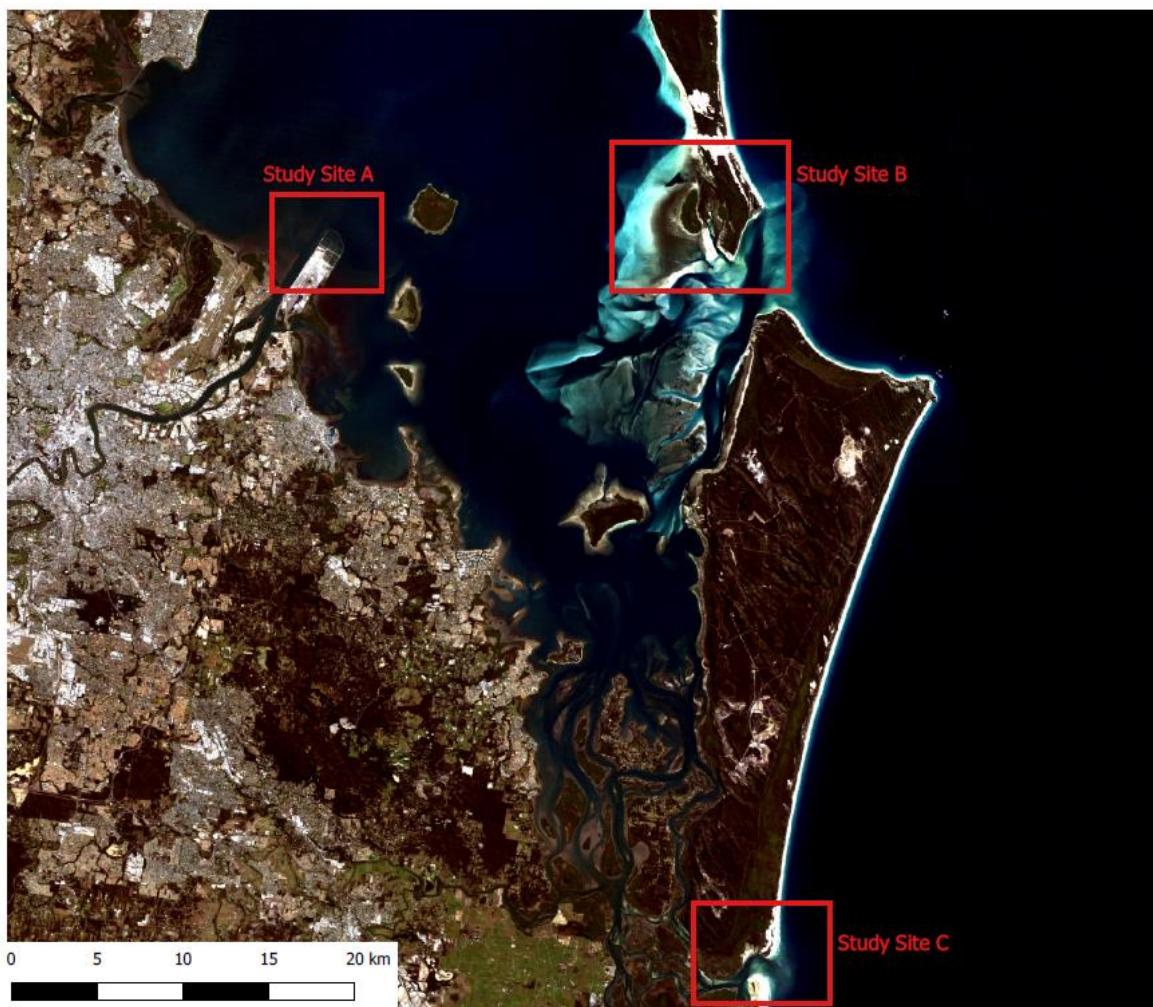


Figure 5 – Moreton Bay, QLD – Study Sites for Change Detection

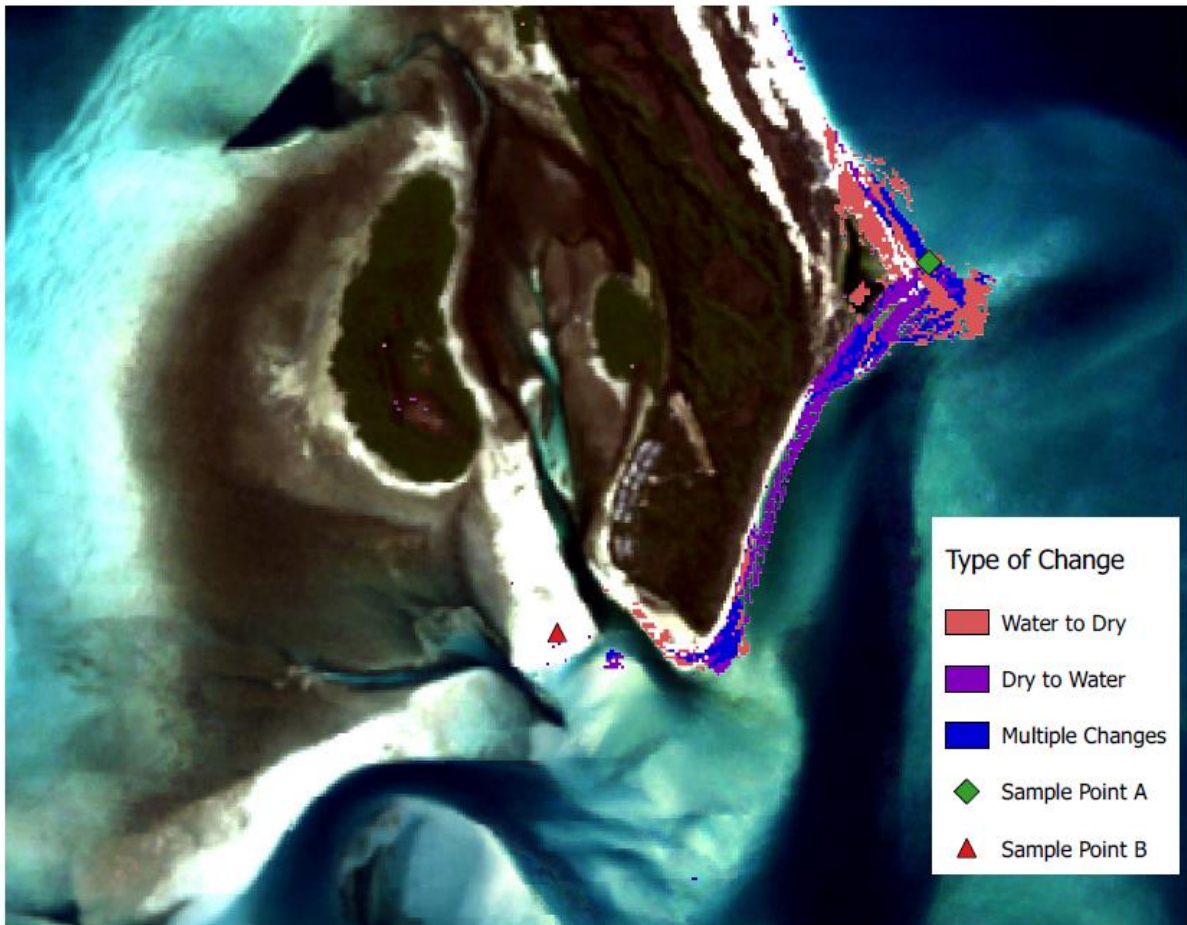


Figure 6 – Southern Moreton Island - 95% Probability of Change areas for Water to Dry, Dry to Water and Multiple Changes. Sample Point locations for multiple (A) and intertidal (B) change analysis.

Here we have been able to not only isolate areas of high change probability from water to dry land and dry land to water, but also the regions where we have observed multiple changes between water to dry land and back again. As the coastline and spatial pattern of sand deposition change dynamically over time (see Appendix A), this is an important feature of the algorithm, but it must also be able to distinguish between more persistent changes and those observed as part of a normal periodic tidal regime. These two types of dynamic change can be examined more closely by querying the time series of results from the random forest water-non water classifier, using the pixel drill tool.

In Figure 7 we see the multiple change pattern observed at Sample Point A, with a clear change to land at this point observed between 1998 and 2002. The uncertainty inherent in defining water from land in these environments is evident in observations after 2002, which may indeed be tidally influenced.

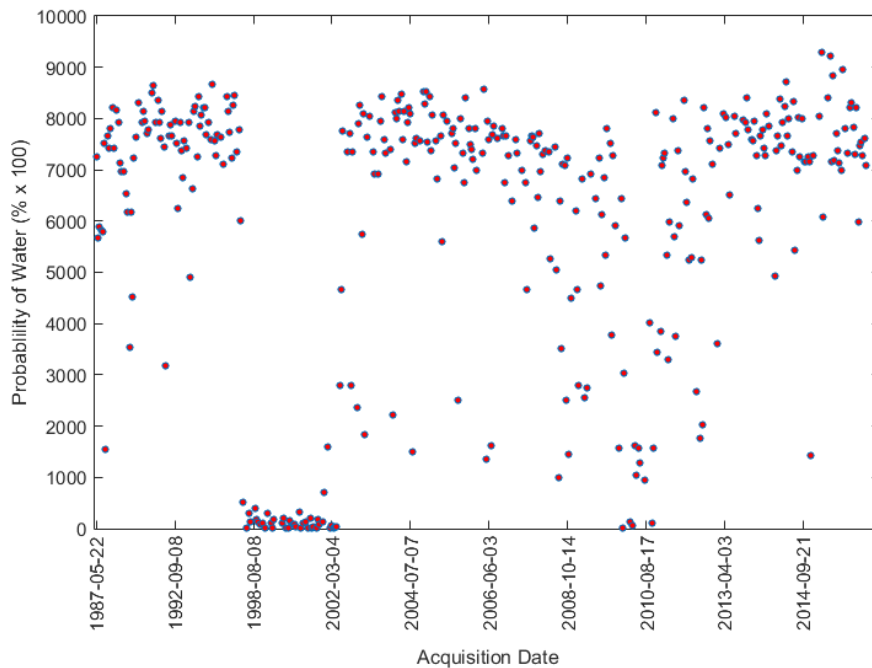


Figure 7 – Pixel Drill at Sample Point A showing Probability of Water detection through the time-series.

The distinct change observed at Point A can be contrasted with the type of change pattern observed at Sample Point B, located in the inter-tidal zone (Figure 8). At this point we observe a periodic drying and inundation of the intertidal zone at the ebb and flow tides. Importantly, the ability to constrain the time window width in the algorithm means these types of short frequency periodic changes don't register as a high change probability in our results. This also means that the window width must be carefully considered, based on the location being analysed, and the specific query being made of the data.

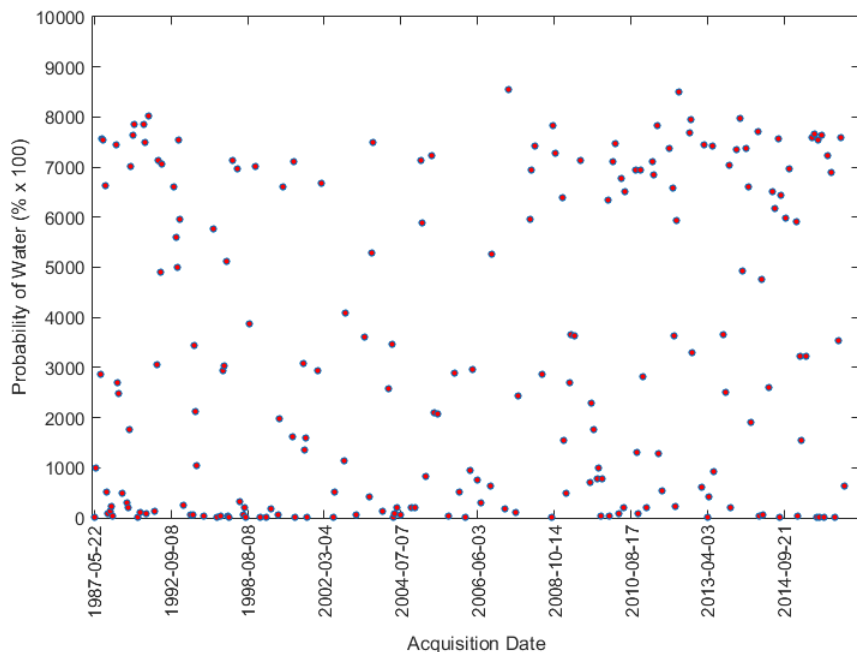


Figure 8 - Pixel Drill at Sample Point B showing Probability of Water detection through the time-series

As shown in the Brisbane Port example, one of the strengths of the algorithm is the ability to not only identify the type and probability of change, but also the time at which it occurred. At study site C at the southern tip of Stradbroke Island, we can examine persistent coastline change events occurring on both sides of the inlet (see also Appendix A)

Figure 9 shows different periods of coastal deposition on the northern and southern sides of the inlet, detected as high probability zones of change from wet to dry.

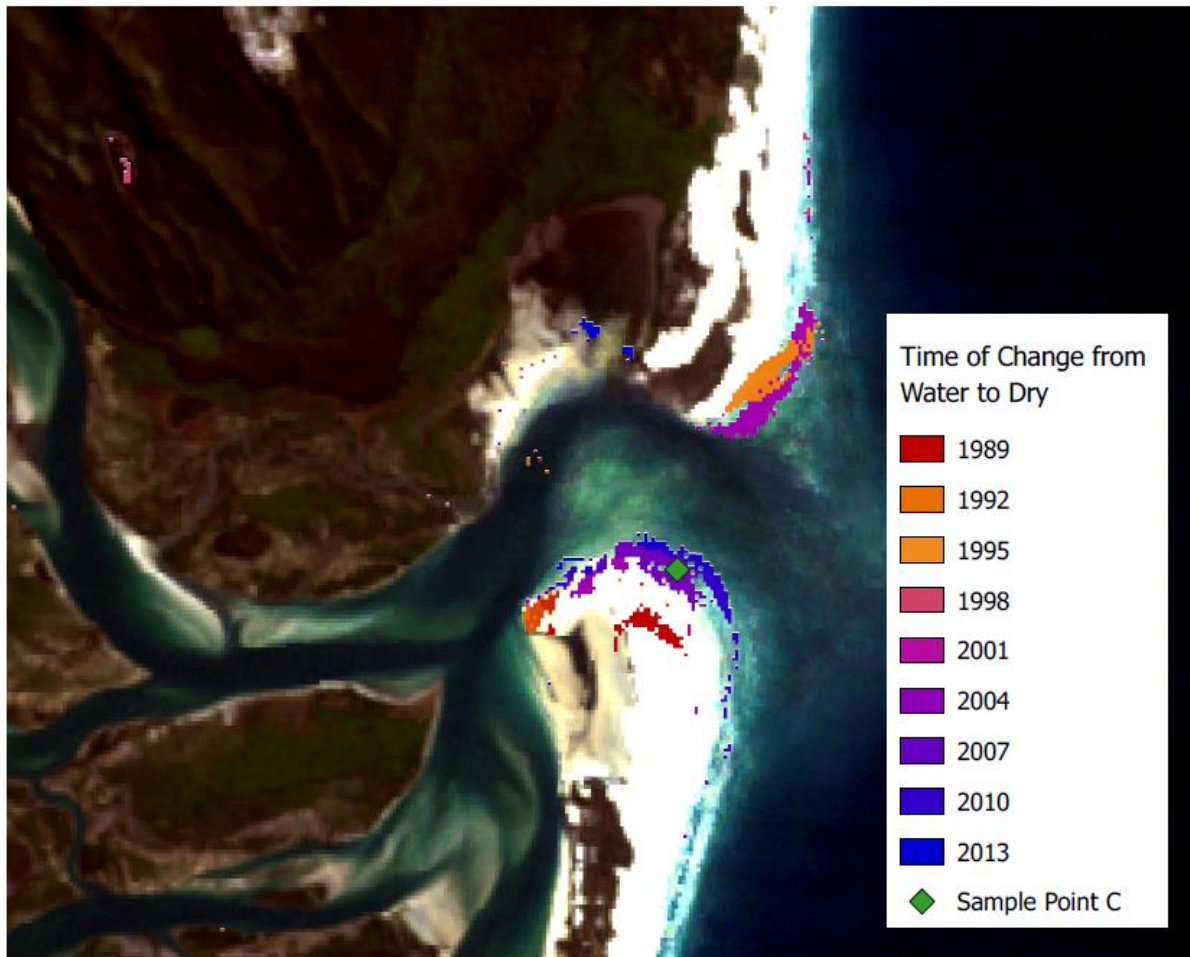


Figure 9 – Southern Stradbroke Island – 95% Probability of Change from Water to Dry and estimated change dates.

We can examine this change through time at Sample Point C using the pixel drill approach (Figure 10). This figure displays a couple of notable features, firstly, the persistent change event in June 2006, falls in the corresponding change period retrieved by the algorithm shown in Figure 9. Secondly, we see some shorter period changes around 1992 and 2002 which are ignored by the algorithm as it searches for persistent change.

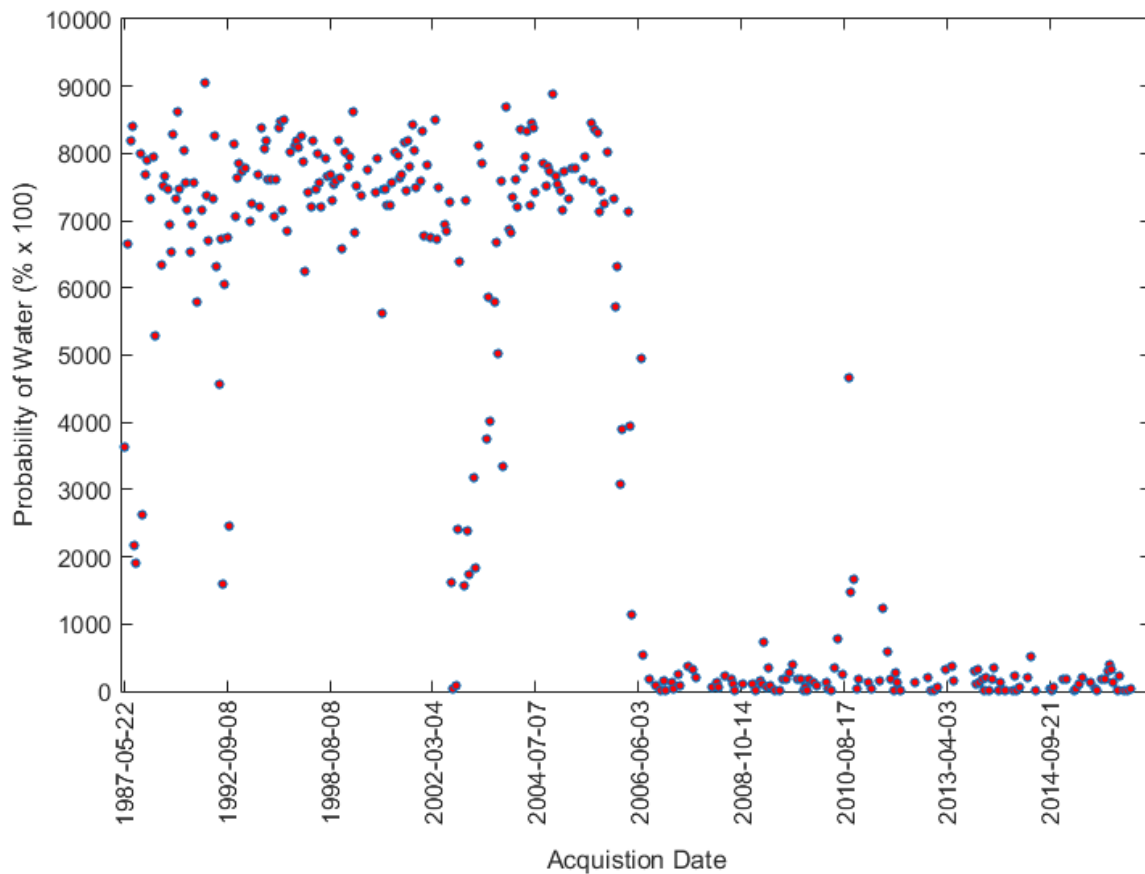


Figure 10 - Pixel Drill at Sample Point C showing Probability of Water detection through the time-series

Looking at the changes from Dry to Wet in this study site (Figure 11) we can see a gradual change over time of the northern section of the inlet as the coastline erodes in towards the lake (see also Appendix A). Again, we can more closely examine the timing and nature of this change by looking through the time series at Sample Point D (Figure 12). Here we see a very distinct change from land to water in approximately 2001, corresponding to the algorithm outputs.

There is a degree of flexibility built into the algorithm, by the ability to tune the temporal window width to detect the types of change the user is looking for. Hence, in conjunction with the use of the pixel drill analysis to estimate a period of change, an iterative approach can be taken if the user wishes to then further examine the spatial extents of the event.

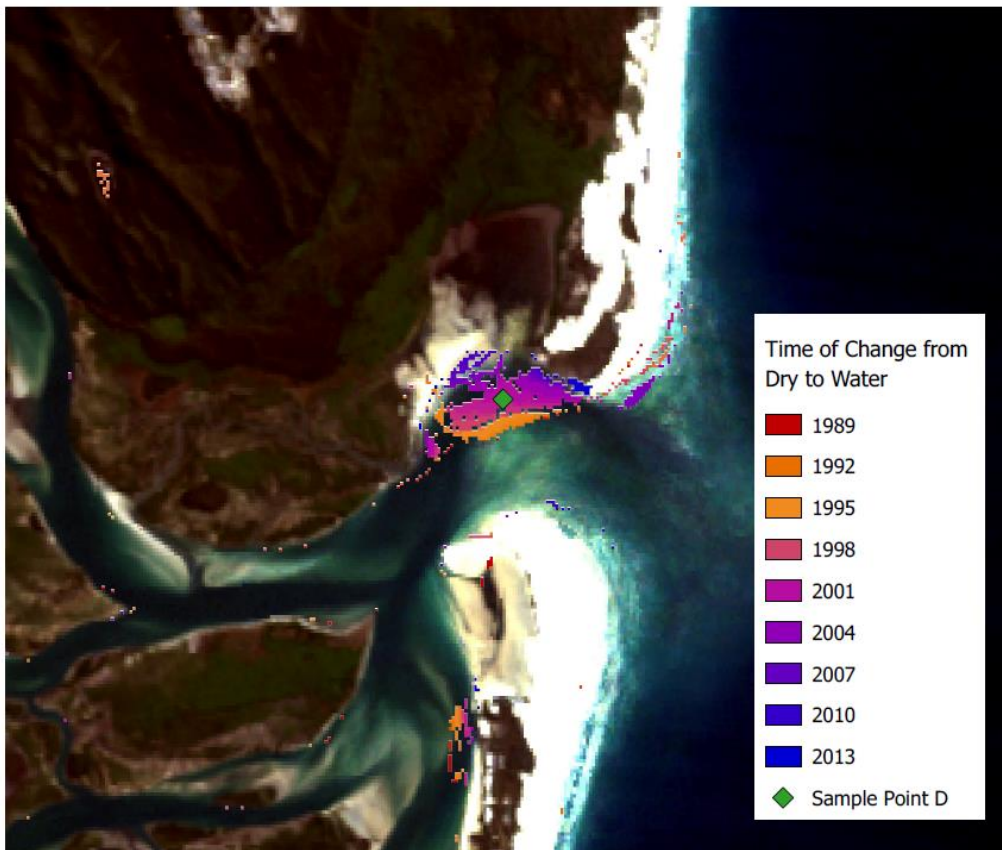


Figure 11 - Southern Stradbroke Island – 95% Probability of Change from Dry to Water and estimated change dates.

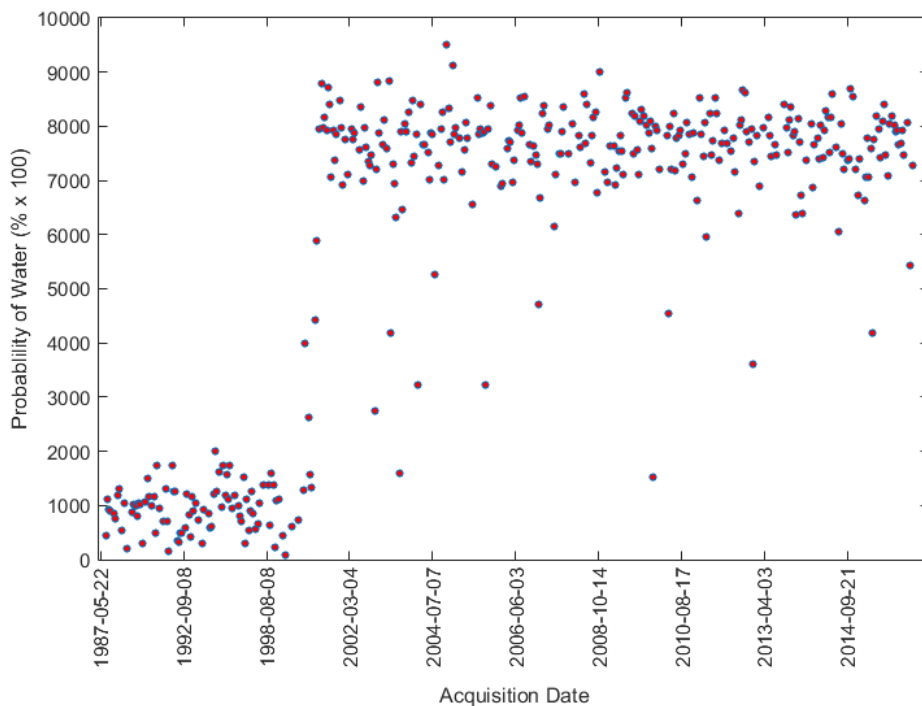


Figure 12 - Pixel Drill at Sample Point D showing Probability of Water detection through the time-series

### 3.2.2 Murray Mouth & Lower Lakes, SA

In this section we test the algorithm on a complex coastal and estuarine system at the mouth of the Murray River in South Australia. This site was selected as it has a number of unique features that enable us to assess different components of the algorithm, and a new method of targeted analysis. Notable features of the site include:

- Distinct boundaries between inland lake and tidal systems, created by the Murray River barrages.
- A specific drying event occurring at the inland lake system during the Millennium drought (MDBA, 2012).
- A highly dynamic river mouth structure, changing significantly over time

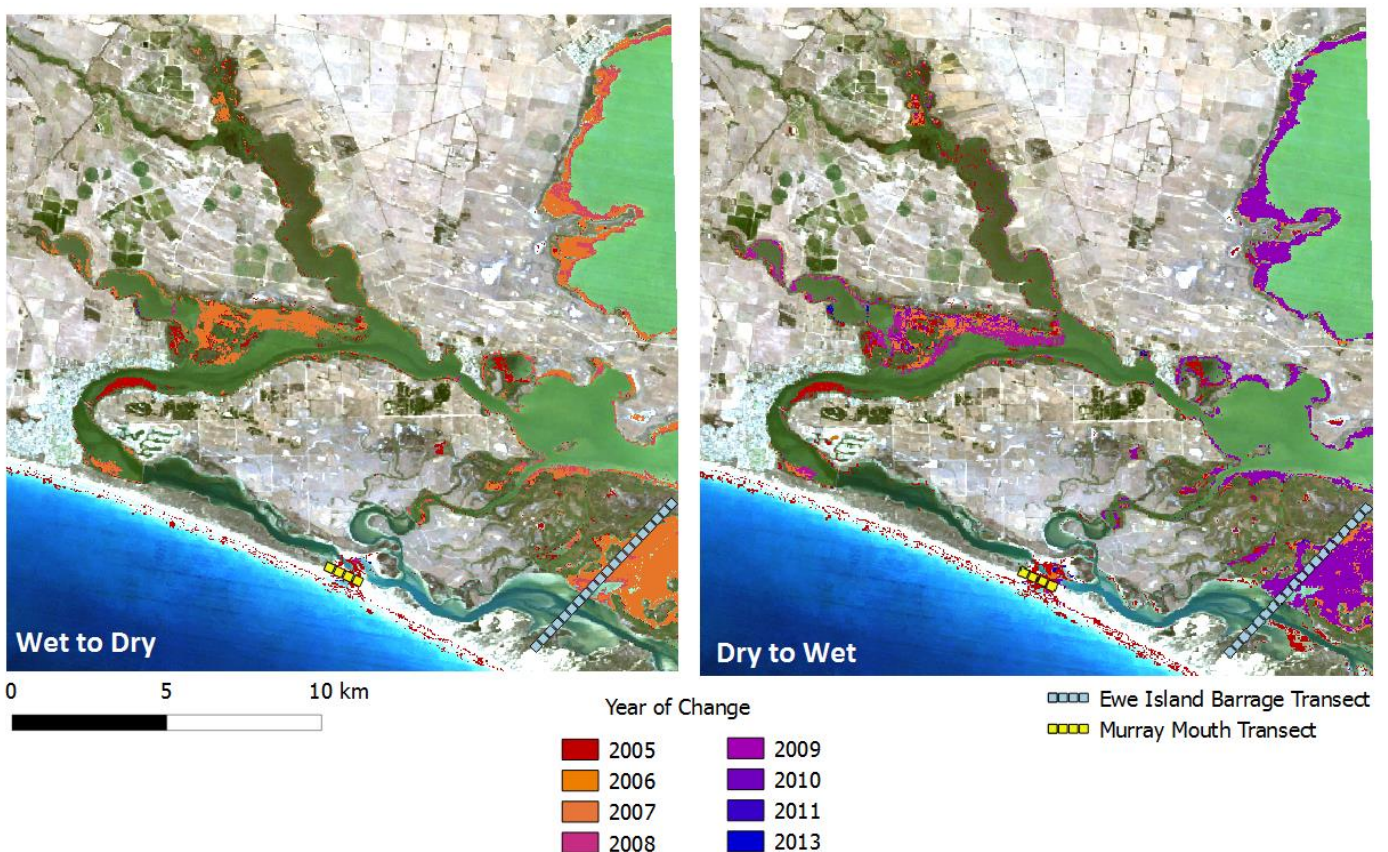


Figure 13 – The Murray Mouth and Lower Lakes Region – 95% Probability of Change regions shown along with the estimated time of change. Transects for further analysis shown over the Murray Mouth and Ewe Island Barrage at Lake Alexandrina

In Figure 13 we can see the diagnostic outputs of the change detection algorithm clearly picking up the widespread drying event in 2006-2007, and as early as 2005 in some lower portions of the river. Subsequent re-inundation of most of these areas then does not occur until 2009-2010. This is consistent with the documented times of drying during the drought (MDBA, 2012). The added benefit of this spatial representation of the time series analysis is the gradual/staged drying around edges of the lake picked up by the algorithm.

To examine the transects shown in Figure 13 we use a tool new to EO data analysis to examine the detected change events, referred to as a Hovmöller diagram (Hovmöller, 1949). Hovmöller diagrams enable a spatio-temporal visualisation of variables over time, and are particularly effective in enabling an intuitive examination of complex events.

For the water/land based change events at this study site, we employ a commonly used water index as an input to the Hovmöller diagrams models. The Normalised Difference Water Index (NDWI) (McFeeters, 1996) is based on a ratio of the observed green and NIR band reflectance values at each pixel:

$$NDWI = \frac{Green - NIR}{Green + NIR}$$

Values of this index range from -1 to 1, with negative values indicating land and positive values indicating water. For our analysis, we calculate the NDWI index for each pixel in each image tile for the time series, before application of the Hovmöller diagram approach.

The Ewe Island barrage is one of five barrages separating the Murray System from the coastal waters of the Coorong (MDBA, 2012). Effectively, this separates the tidal coastal system and the River and Lake system that was severely affected by the drought drying event. We can examine this spatial relationship using the NDWI time series as shown in Figure 14.

Figure 14 clearly displays the drying event that occurred in Lake Alexandrina commencing in late 2006 and then extending all the way to the barrage (transect pixel 120) at the beginning of 2007. The end of the drought is reflected by the inundation of the lake areas (Pixels 30 to 120) at the end of 2009. The diagram also highlights clearly the periodic nature of the tidally influenced regions south of the barrage, with the regular nature of the drying and inundation events shown from pixels 120 to 165).

Our results can be correlated to river flow data (Figure 15) obtained from Lock One, managed by the Murray Darling Basin Authority (MDBA) and supplied through the SA Department of Environment, Water and Natural Resources (<https://www.waterconnect.sa.gov.au/Systems/SiteInfo/Pages/Default.aspx?site=A4260903&period=HRLY#HistoricData>)

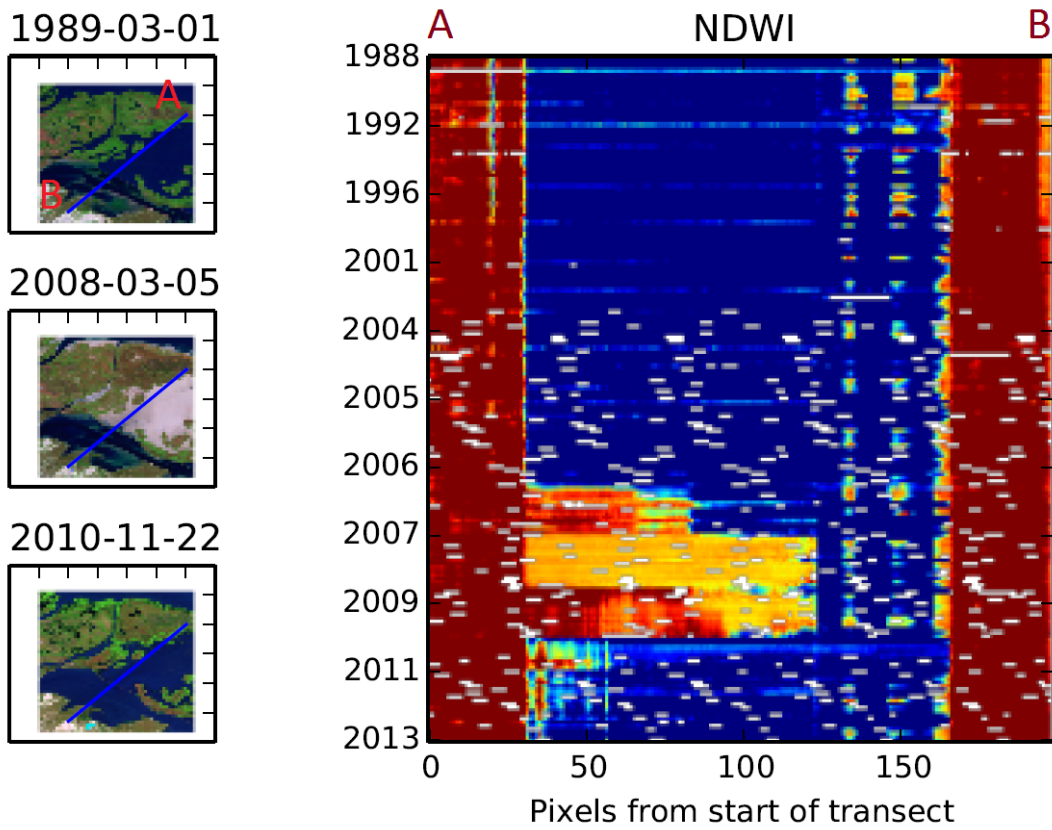


Figure 14 – Hovmöller Diagram of the Ewe Island Barrage Transect. Low NDWI values (red) indicate Land, through to high values (blue) indicating water.

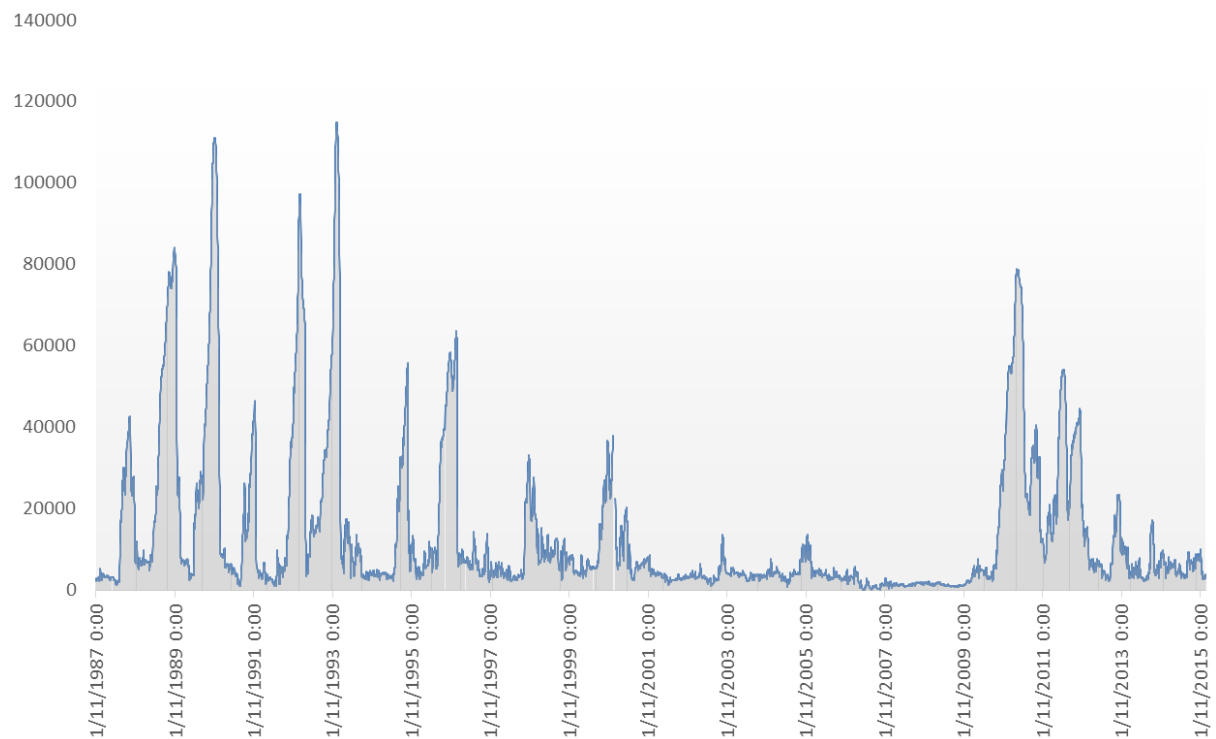


Figure 15 – River Flow Data at River Murray Lock One Downstream – Megalitres per Day.

Here we clearly see greatly reduced river flows commencing from 2001, before a further significant reduction in 2006/2007, closely correlated to the largest spatial extent of drying seen in Figure 14. The abrupt increase in flow in 2009/10 is again mirrored in the results of the time series analysis, with the release of water through the barrage. This increased flow damped the tidal regime for this short period on the southern side of the barrage (pixels ~ 120-165).

At the Murray Mouth Transect we examine the movement of the Murray Mouth structure, again through using the NDWI index and time series analysis using the Hovmöller diagram. Figure 16 shows the dynamic nature of both the size and position of the mouth over the full extent of the time series.

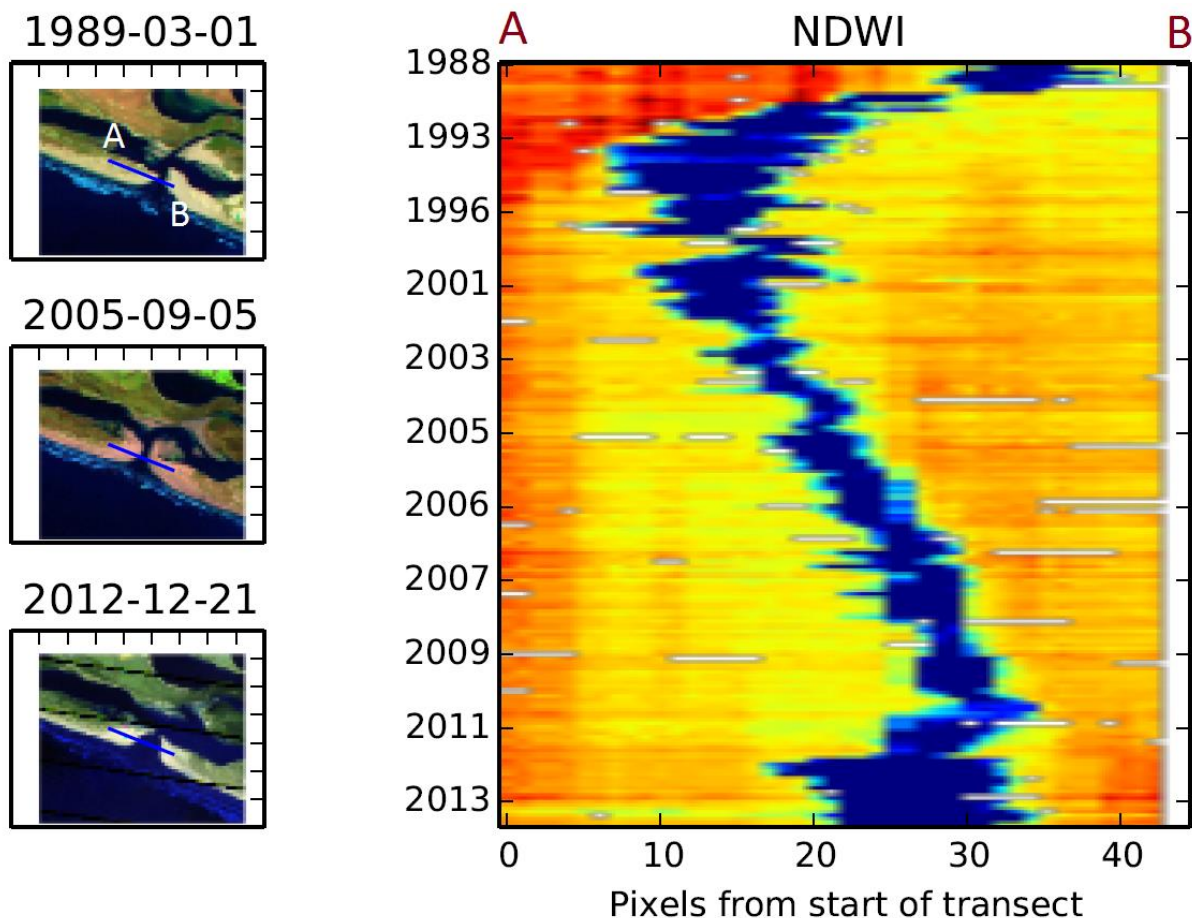


Figure 16 - Hovmöller Diagram of the Murray Mouth Transect. Low NDWI values (red) indicate Land, through to high values (blue) indicating water

Here we can clearly see the narrowing and widening of the river mouth as it changes position over time, including instances in 1990, 1997 and 2002 when it nearly closes entirely at this location. The effect of the dredging that then took place between 2002 and 2010 to ensure the mouth remains open (Water and Natural Resources (DEWNR), 2015) is reflected by the wider river mouth across this period. The full dynamic nature of the mouth can also be viewed in the accompanying video detailed in Appendix A.

## 4. FUTURE WORK & LINKAGES

In this section we look at two important ecological communities that could be examined using the time series change detection algorithm we have developed, and the associated tools that enable a more detailed interrogation of change events and trends.

### 4.1 Extension to other Variables

One important ecological community that can be examined by the application of indices and the time-series analysis approach is mangroves. The use of the Normalised Difference Vegetation (NDVI) index can indicate the health of mangrove communities through the time-series, and clearly indicate change.

In the example below we examine a transect through the Junction Bay mangrove community in the Northern Territory. This estuary is of particular interest from a change detection perspective, due to the impact of two tropical cyclones, TC Debbie (Cat 3 in 2003) and TC Monica (Cat 5 in 2006). In Figure 17 we see the damage caused directly after TC Monica.



Figure 17 – Junction Bay mangrove community stripped and flattened, post TC Monica– Photo Credit: Garry Cook, CSIRO Sustainable Ecosystems

Examining the transect displayed in the Hovmöller diagram, we clearly see the decrease in vegetation health after severe TC Monica in 2006. From this analysis, it is clear that the community has yet to fully recover to its previous condition even 7-8 years after the event. It is this kind of feature of the time series approach that could prove very valuable to ecosystem monitoring, as we can not only isolate the change event, but the longer term associated effects.

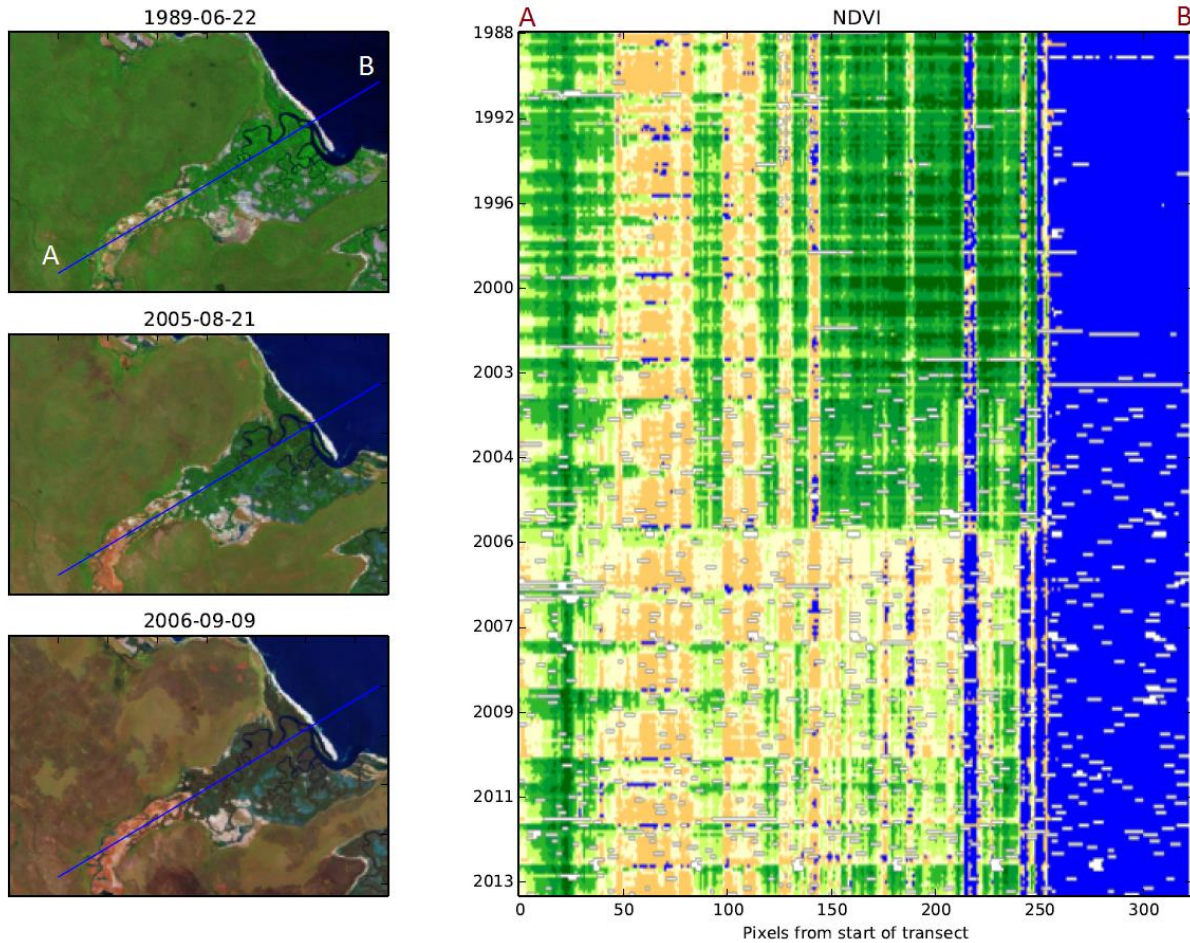


Figure 18 - Hovmöller Diagram of the Junction Bay Mangrove Community, NT. High NDVI values (green) indicate healthy vegetation, through to yellow which is indicative of soil or damaged vegetation, through to blue indicating water.

Whilst we can explore change events based on indices and spectral data such as the mangrove example above, the change detection algorithm is designed to interpret classified objects, and hence could be extended to any environment class that can be reliably classified from EO data.

Saltmarsh communities are also important under The Environmental Protection and Biodiversity Conservation (EPBC) Act managed by the Department of the Environment. In particular, Subtropical and Temperate Coastal Saltmarsh are listed as vulnerable under the Act. Provided relevant field observations/ecological expertise can be brought to the classification of these communities based on EO data, the change detection algorithm in this

report could provide a framework for developing baselines and monitoring change in their extent.

This kind of mapping and monitoring also has the potential to complement research being conducted in Project B4 of the NESP (Underpinning the repair and conservation of Australia's threatened coastal marine habitats), by providing baselines, robust measures of past change and monitoring to support efforts for the rehabilitation of estuarine/coastal habitats.

## 4.2 Developing Data Sets to support Coastal Applications

GA is currently developing workflows to extract statistical surface reflectance composites from the Landsat archive data in the AGDC, based on a range of physical indices (e.g NDVI) and seasonal epochs.

For our work in this aquatic/coastal space, we have established a database of tidal offsets relative to MSL for each coastal tile in the AGDC based on the time of acquisition, utilising the OTPS tidal models developed at Oregon State University ([http://volkov.oce.orst.edu/tides/tpxo8\\_atlas.html](http://volkov.oce.orst.edu/tides/tpxo8_atlas.html)).

As part of evaluating these tidal models, we are producing first pass composite median reflectance images of the Australian coastline at both low and high observed tide across 20 years of the Landsat archive in the AGDC. The current version is derived using an independent spectral band based median approach, creating a synthetic spectra, however a number of methods can be employed to create the composite spectra.

Once developed, these cloud and noise free data sets have significant potential to improve habitat classification, change detection and feature delineation in the coastal zone, and can be derived over a used defined range of seasonal, tidal or finer-scale temporal epochs. In Figure 19 we show an example of such imagery derived at high and low tide in the Kimberley region of WA.

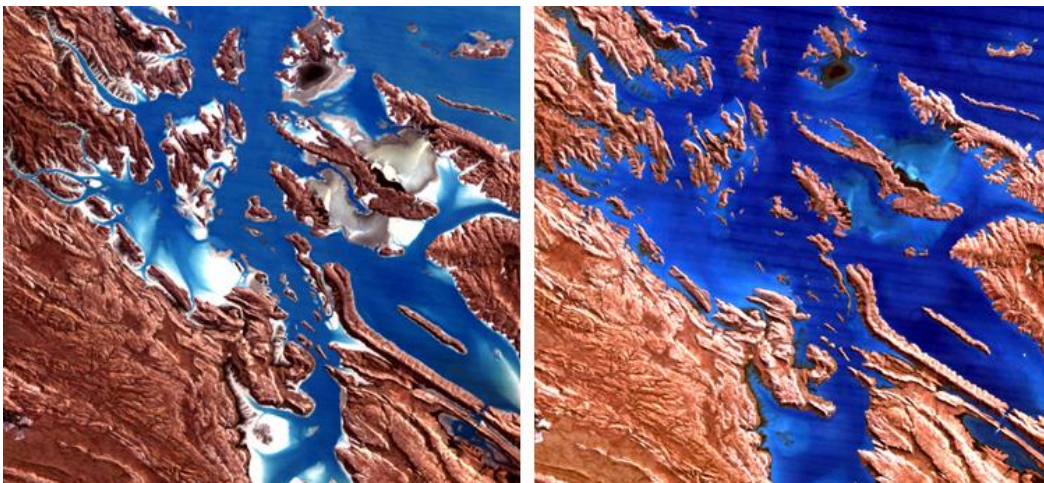


Figure 19 – Low (left) and High (right) tide composite reflectance images derived from modelled tides across 20 years of Landsat data in the Kimberley Region, WA.

## 5. CONCLUSIONS

In this report we have focused on the detection of water from Landsat EO data held in the AGDC, as a method for extending current EO work at Geoscience Australia into coastal change detection. However, the change detection algorithm we have described has been designed so it can be applied to any variable that can be classified using EO data across the coastal zone. This flexibility is key to the usability of the algorithm, and its potential for further use in coastal projects and linkages with other government environmental priorities.

The broad scale diagnostic properties of the algorithms allow the full 28 years of Earth Observation data to be examined, without prior knowledge of a specific change extent or timing. Once change is identified, we have demonstrated further tools that can then be applied to examine more specifically the nature of the change event

Future work in this space could aid in mapping and monitoring the distribution of threatened communities, habitat change from extreme events, and the change over time of important ecological communities such as mangroves and salt marshes.

## REFERENCES

- Breiman, L., 2001. Random Forests. *Mach. Learn.* 45, 5–32. doi:10.1023/A:1010933404324
- Brockmann, C., Stelzer, K., 2008. Optical Remote Sensing of Intertidal Flats, in: Barale, V., Gade, M. (Eds.), *Remote Sensing of the European Seas*. Springer Netherlands, pp. 117–128.
- Chen, L.C., Rau, J.Y., 1998. Detection of shoreline changes for tideland areas using multi-temporal satellite images. *Int. J. Remote Sens.* 19, 3383–3397.
- Fisher, A., Danaher, T., 2013. A Water Index for SPOT5 HRG Satellite Imagery, New South Wales, Australia, Determined by Linear Discriminant Analysis. *Remote Sens.* 5, 5907–5925. doi:10.3390/rs5115907
- Fisher, A., Flood, N., Danaher, T., 2016. Comparing Landsat water index methods for automated water classification in eastern Australia. *Remote Sens. Environ.* 175, 167–182. doi:10.1016/j.rse.2015.12.055
- Ho, T.K., 1995. Random decision forests, in: *Proceedings of the Third International Conference on Document Analysis and Recognition, 1995*. Presented at the Proceedings of the Third International Conference on Document Analysis and Recognition, 1995, pp. 278–282 vol.1. doi:10.1109/ICDAR.1995.598994
- Hovmöller, E., 1949. The Trough-and-Ridge diagram. *Tellus* 1, 62–66. doi:10.1111/j.2153-3490.1949.tb01260.x
- Lewis, A., Lymburner, L., Purss, M.B.J., Brooke, B., Evans, B., Ip, A., Dekker, A.G., Irons, J.R., Minchin, S., Mueller, N., Oliver, S., Roberts, D., Ryan, B., Thankappan, M., Woodcock, R., Wyborn, L., 2015. Rapid, high-resolution detection of environmental change over continental scales from satellite data – the Earth Observation Data Cube. *Int. J. Digit. Earth* 0, 1–6. doi:10.1080/17538947.2015.1111952
- Li, F., Jupp, D.L.B., Thankappan, M., Lymburner, L., Mueller, N., Lewis, A., Held, A., 2012. A physics-based atmospheric and BRDF correction for Landsat data over mountainous terrain. *Remote Sens. Environ.* 124, 756–770. doi:10.1016/j.rse.2012.06.018
- Lyons, M.B., Phinn, S.R., Roelfsema, C.M., 2012. Long term land cover and seagrass mapping using Landsat and object-based image analysis from 1972 to 2010 in the coastal environment of South East Queensland, Australia. *ISPRS J. Photogramm. Remote Sens.* 71, 34–46. doi:10.1016/j.isprsjprs.2012.05.002
- McFeeters, S.K., 1996. The use of the Normalized Difference Water Index (NDWI) in the delineation of open water features. *Int. J. Remote Sens.* 17, 1425–1432. doi:10.1080/01431169608948714
- MDBA, 2012. Fact Sheet - All About the Barrages (No. MDBA Publication 24/11). Murray Darling Basin Authority.
- Mueller, N., Lewis, A., Roberts, D., Ring, S., Melrose, R., Sixsmith, J., Lymburner, L., McIntyre, A., Tan, P., Curnow, S., Ip, A., 2016. Water observations from space: Mapping surface water from 25 years of Landsat imagery across Australia. *Remote Sens. Environ.* 174, 341–352. doi:10.1016/j.rse.2015.11.003
- Murray, N.J., Clemens, R.S., Phinn, S.R., Possingham, H.P., Fuller, R.A., 2014. Tracking the rapid loss of tidal wetlands in the Yellow Sea. *Front. Ecol. Environ.* 12, 267–272. doi:10.1890/130260
- Murray, N.J., Phinn, S.R., Clemens, R.S., Roelfsema, C.M., Fuller, R.A., 2012. Continental Scale Mapping of Tidal Flats across East Asia Using the Landsat Archive. *Remote Sens.* 4, 3417–3426. doi:10.3390/rs4113417
- Ryu, J.-H., Won, J.-S., Min, K.D., 2002. Waterline extraction from Landsat TM data in a tidal flat: A case study in Gomso Bay, Korea. *Remote Sens. Environ.* 83, 442–456. doi:10.1016/S0034-4257(02)00059-7

- Shetty, A., Jayappa, K.S., Mitra, D., 2015. Shoreline Change Analysis of Mangalore Coast and Morphometric Analysis of Netravathi-Gurupur and Mulky-pavanje Spits. *Aquat. Procedia*, INTERNATIONAL CONFERENCE ON WATER RESOURCES, COASTAL AND OCEAN ENGINEERING (ICWRCOE'15) 4, 182–189.  
doi:10.1016/j.aqpro.2015.02.025
- Sixsmith, J., Oliver, S., Lymburner, L., 2013. A hybrid approach to automated landsat pixel quality, in: *Geoscience and Remote Sensing Symposium (IGARSS), 2013 IEEE International*. Presented at the Geoscience and Remote Sensing Symposium (IGARSS), 2013 IEEE International, pp. 4146–4149.  
doi:10.1109/IGARSS.2013.6723746
- Tan, P., Lymburner, L., Thankappan, M., Lewis, A., 2011. Mapping Cropping Practices Using MODIS Time Series: Harnessing the Data Explosion. *J. Indian Soc. Remote Sens.* 39, 365–372. doi:10.1007/s12524-011-0124-0
- Tulbure, M.G., Broich, M., Stehman, S.V., Kommareddy, A., 2016. Surface water extent dynamics from three decades of seasonally continuous Landsat time series at subcontinental scale in a semi-arid region. *Remote Sens. Environ.* 178, 142–157.  
doi:10.1016/j.rse.2016.02.034
- Verbesselt, J., Hyndman, R., Zeileis, A., Culvenor, D., 2010. Phenological change detection while accounting for abrupt and gradual trends in satellite image time series. *Remote Sens. Environ.* 114, 2970–2980. doi:10.1016/j.rse.2010.08.003
- Water and Natural Resources (DEWNR), 2015. Keeping the Murray Mouth open [WWW Document]. URL <http://www.naturalresources.sa.gov.au/samurraydarlingbasin/projects/all-projects-map/keeping-the-murray-mouth-open> (accessed 4.13.16).
- White, K., El Asmar, H.M., 1999. Monitoring changing position of coastlines using Thematic Mapper imagery, an example from the Nile Delta. *Geomorphology* 29, 93–105.  
doi:10.1016/S0169-555X(99)00008-2
- Xu, H., 2006. Modification of normalised difference water index (NDWI) to enhance open water features in remotely sensed imagery. *Int. J. Remote Sens.* 27, 3025–3033.  
doi:10.1080/01431160600589179
- Yamano, H., Tamura, M., 2004. Detection limits of coral reef bleaching by satellite remote sensing: Simulation and data analysis. *Remote Sens. Environ.* 90, 86–103.  
doi:10.1016/j.rse.2003.12.005

## APPENDIX A

Included as Appendices to this work are links to the metadata records and download links for short movies visualising the times-series of Landsat images used to complete analysis at the following sites:

Study Site B – Southern\_Moreton\_Island.mp4

Metadata: <http://catalogue.aodn.org.au/geonetwork/srv/eng/metadata.show?uuid=90f1121e-b973-46d4-9a51-5f750d954319>

Video: [http://data.imas.utas.edu.au/attachments/90f1121e-b973-46d4-9a51-5f750d954319/steve%20sagar%20-%20Southern\\_Moreton\\_Island.mp4](http://data.imas.utas.edu.au/attachments/90f1121e-b973-46d4-9a51-5f750d954319/steve%20sagar%20-%20Southern_Moreton_Island.mp4)

Study Site C – Southern\_Stradbroke\_Island.mp4

Metadata: <http://catalogue.aodn.org.au/geonetwork/srv/eng/metadata.show?uuid=67fef6b1-1540-445f-a995-71abcefeb99b>

Video: [http://data.imas.utas.edu.au/attachments/67fef6b1-1540-445f-a995-71abcefeb99b/steve%20sagar%20-%20Southern\\_Stradbroke\\_Island.mp4](http://data.imas.utas.edu.au/attachments/67fef6b1-1540-445f-a995-71abcefeb99b/steve%20sagar%20-%20Southern_Stradbroke_Island.mp4)

The Murray Mouth – MurrayMouth.mp4

Metadata: <http://catalogue.aodn.org.au/geonetwork/srv/eng/metadata.show?uuid=a0bf5d29-0986-443a-a9e2-a9d7523c9a3c>

Video: <http://data.imas.utas.edu.au/attachments/a0bf5d29-0986-443a-a9e2-a9d7523c9a3c/steve%20sagar%20-%20MurrayMouth.wmv>



[www.nespmarine.edu.au](http://www.nespmarine.edu.au)

Contact:  
Stephen Sagar  
Geoscience Australia

GPO Box 378 Canberra ACT 2601  
[stephen.sagar@ga.gov.au](mailto:stephen.sagar@ga.gov.au) | tel +61 2 6249 9877